

Spin-orbit fields in asymmetric (001) quantum wells

P. S. Eldridge,^{1,*} J. Hübner,¹ S. Oertel,¹ R. T. Harley,² M. Henini,³ and M. Oestreich¹

¹*Institute for Solid State Physics, Leibniz University of Hannover, Appelstr. 2, 30167 Hannover, Germany*

²*School of Physics and Astronomy, University of Southampton, Southampton, SO17 1BJ, UK*

³*School of Physics and Astronomy, University of Nottingham, Nottingham, NG7 4RD, UK*

(Dated: May 24, 2021)

We measure simultaneously the in-plane electron g-factor and spin relaxation rate in a series of undoped inversion-asymmetric (001)-oriented GaAs/AlGaAs quantum wells by spin-quantum beat spectroscopy. In combination the two quantities reveal the absolute values of both the Rashba and the Dresselhaus coefficients and prove that the Rashba coefficient can be negligibly small despite huge conduction band potential gradients which break the inversion symmetry. The negligible Rashba coefficient is a consequence of the ‘isomorphism’ of conduction and valence band potentials in quantum systems where the asymmetry is solely produced by alloy variations.

PACS numbers: 71.70.Ej, 72.25.Fe, 72.25.Rb, 73.21.Fg

Symmetry is a thread which runs through all of physics and symmetry reduction discloses basic physical principles. In this letter, we employ crystallographically engineered symmetry reduction to study the intricate effects of spin-orbit interaction on the electron spin in semiconductor nanostructures. Symmetry reduction is an especially powerful tool in semiconductor physics because the variety of crystallographic directions combined with bandgap engineering allow enormous freedom.

The interplay between structure, symmetry and electron spin in semiconductors directly affects the spin relaxation rate Γ_s and the effective electron Landé-factor g . Early studies of Γ_s and g were focused on bulk zincblende material where both entities are isotropic [1]. Subsequently, the reduction in symmetry from T_d to D_{2d} symmetry in symmetrical (001)-oriented quantum wells (QWs) was shown to give rise to anisotropy between the in-plane (x,y) and the out of plane (z) directions [2, 3]. Further reduction in symmetry to C_{2v} is achieved in (001) quantum wells by removing the mirror symmetry of the quantum well potential and allows an in-plane, two-fold symmetric anisotropy of both Γ_s [4] and g [5].

Fundamentally, Γ_s and g are both determined by spin-orbit interaction but the basic mechanisms for their anisotropies are quite different. Theoretically the in-plane anisotropy of g is proportional to the asymmetry of the electron wavefunction in the growth direction with proportionality constant given by the Dresselhaus or bulk inversion asymmetry (BIA) spin-splitting coefficient γ [5, 6]. In contrast, Γ_s is in many cases dominated by the Dyakonov-Perel spin-relaxation mechanism and the related in-plane anisotropy depends on the ratio (α/β) of the Rashba structural inversion asymmetry (SIA) to the BIA spin splitting [4]. The SIA component is determined in a rather subtle way by the asymmetry of the *structure* along the growth direction [7, 8].

In this letter, we determine the absolute value of both the Rashba and Dresselhaus coefficients for a series of quantum well structures by simultaneously measuring

the in-plane anisotropy of Γ_s and g by spin quantum beat spectroscopy [9]. The specially designed undoped (001) quantum well samples, with reduced C_{2v} symmetry but *without* external electric fields, illustrate clearly the different origins of the two anisotropies as they possess a strong anisotropy of g and nearly negligible anisotropy of Γ_s .

Anisotropies of Γ_s and g have been measured previously in symmetrically grown quantum wells in an external electric field [10, 11] but the decisive simultaneous evaluation of Dresselhaus and Rashba components has not been carried out so far. Hanle experiments in undoped asymmetric quantum wells without an applied electric field have revealed a strong in-plane anisotropy of the Hanle depolarization curve [12] but such measurements are unable to distinguish between anisotropy of Γ_s and g [13]. Recently, Ganichev and co-workers introduced a seminal technique that uses the angular distribution of the spin-galvanic effect and therewith measured the *ratio* of the Rashba and Dresselhaus coefficients in doped quantum wells [14, 15]. Salis and co-workers developed a technique that in principle yields the absolute values of the coefficients in doped structures by optically monitoring the angular dependence of the electrons spin precession [16]. However as the calculation of electric fields in these samples is complicated the values of the coefficients can be overestimated [17].

We first summarise the theoretical mechanisms for g and Γ_s anisotropy [4, 5]. For g a small magnetic field in x -direction B_x deflects the rapid zero-point motion of an electron quantized in z -direction and yields a change of momentum in y -direction. This additional momentum δp_y changes the effective Rashba Ω_R and Dresselhaus Ω_D precession vectors which read for (001) quantum wells in zinc-blend crystals

$$\Omega_R(\mathbf{p}) = \alpha/\hbar^2 \begin{pmatrix} p_y \\ -p_x \\ 0 \end{pmatrix} \quad \Omega_D(\mathbf{p}) = \beta/\hbar^2 \begin{pmatrix} -p_x \\ p_y \\ 0 \end{pmatrix} \quad (1)$$

where α and β are coefficients and $p_{x,y,z}$ are the components of the electron momentum. Inspection of Eq. 1 shows that the Rashba term converts δp_y into an additional magnetic field which is parallel to the external magnetic field B_x and thereby alters the diagonal component of the g-tensor ($g_{xx} = g_{yy}$). By contrast, the Dresselhaus term $\Omega_{\mathbf{D}}$ converts δp_y to an additional magnetic field in y-direction, i.e. perpendicular to B_x and thereby generates an off-diagonal component g_{xy} . A rigorous theoretical treatment yields [5]

$$g_{xy} = g_{yx} = (2\gamma e/\hbar^3 \mu_B) (\langle p_z^2 \rangle \langle z \rangle - \langle p_z^2 z \rangle), \quad (2)$$

where μ_B is the Bohr magneton and $\langle \rangle$ represents an expectation value for the electron wavefunction. The two terms in Eq. 2 cancel and g_{xy} vanishes if the electron wavefunction is symmetric. The anisotropy of the g-tensor is thus proportional to the Dresselhaus coefficient γ and determined by asymmetry of the electron wavefunction which may be induced by asymmetry of the confining (conduction band) potential for the electrons. The effective g-factor for magnetic field oriented at angle ϕ to the (110) axis in the quantum well plane is given by

$$g(\phi) = -\sqrt{g_{xx}^2 + g_{yy}^2 + 2g_{xx}g_{xy} \sin(2\phi)}. \quad (3)$$

For the spin relaxation which is dominated by the Dyakonov-Perel mechanism the rate in the quantum well plane $\Gamma_s^{xy}(\phi)$ is proportional to $\langle \Omega^2 \rangle$ where $\Omega = \Omega_{\mathbf{D}} + \Omega_{\mathbf{R}}$, the sum of Dresselhaus and Rashba components. It will be anisotropic as a result of interference of the components and is given by [4]

$$\Gamma_s^{xy}(\phi) = \frac{C}{2}(\alpha^2 + \beta^2 + 2\alpha\beta \sin(2\phi)),$$

where C is a constant which depends on the in-plane electron momentum relaxation time which is not well known in general. Thus, the spin relaxation rate anisotropy gives the ratio α/β , where $\beta = \langle p_z^2 \rangle > \gamma/\hbar^2$.

Experimentally, we measure the electron spin relaxation rate along the growth direction (z) for a magnetic field applied in the quantum well plane. The magnetic field causes rapid Larmor precession of the electron spins about the magnetic field and the measured relaxation rate is given by the average of $\Gamma_s^z = C(\alpha^2 + \beta^2)$ and $\Gamma_s^{xy}(\phi)$ [11]:

$$\Gamma_s(\phi) = \frac{1}{2}(\Gamma_s^z + \Gamma_s^{xy}(\phi)) = D \left[1 + \left(\frac{\alpha}{\beta} \right)^2 + \frac{2\alpha}{3\beta} \sin(2\phi) \right] \quad (4)$$

where $D = 3C\beta^2/4$. Therefore measurement of both anisotropies yields simultaneously the absolute values of α and β . It is interesting to note that spin relaxation rate anisotropy has the same form as the g-factor but with β replacing g_{xx} and α replacing g_{xy} .

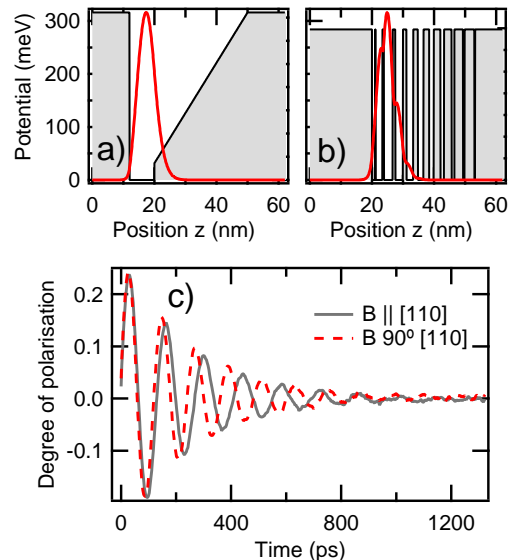


FIG. 1: (Color online) Conduction band potential profile and numerical calculated electron wavefunction for the $n = 1$ states for a) sample A and b) sample B. c) The measured spin quantum beats at 125 K for sample A for 3 T in-plane magnetic field clearly showing the different electron g-factors for $B||[110]$ and $[1\bar{1}0]$ and similar spin relaxation times.

The samples are four molecular beam epitaxy grown, (001)-oriented GaAs/AlGaAs multiple quantum wells with varying asymmetry. Sample A comprises 5 repeats of a 12 nm $\text{Al}_{0.4}\text{Ga}_{0.6}\text{As}$ barrier, an 8 nm GaAs quantum well followed by a 30 nm alloy layer where the aluminium concentration is varied linearly from 0.04 to 0.4. Samples B-D are equivalent structures but the one sided potential gradient is in the quantum well and has been grown as digital alloy with conduction band gradients equivalent to an electric field of 100 kV/cm for sample B, 50 kV/cm for sample C, and 25 kV/cm for sample D. Figure 1 shows the calculated $n=1$ electron states for samples A and B obtained by numerical solution of the Schrödinger equation. The calculated confinement energies for electrons in samples A to D are 34 meV, 91 meV, 61 meV and 37 meV, respectively.

The samples are mounted on a rotation stage in a liquid helium flow cryostat in a superconducting magnet with the magnetic field oriented in Voigt geometry. The rotation axis corresponds to the growth axis of the sample and is parallel to the direction of excitation. Spin oriented electrons are optically created by circularly polarized picosecond pulses from a mode-locked Ti:Sapphire laser with a repetition rate of 80 MHz, a laser wavelength of 740 nm and a pulse intensity yielding excitation density $\approx 2 \times 10^{10} \text{ cm}^{-2}$. After excitation the carrier momentum distribution rapidly thermalizes by emission of phonons and scattering with other carriers and the holes lose their spin orientation within the momentum relaxation time

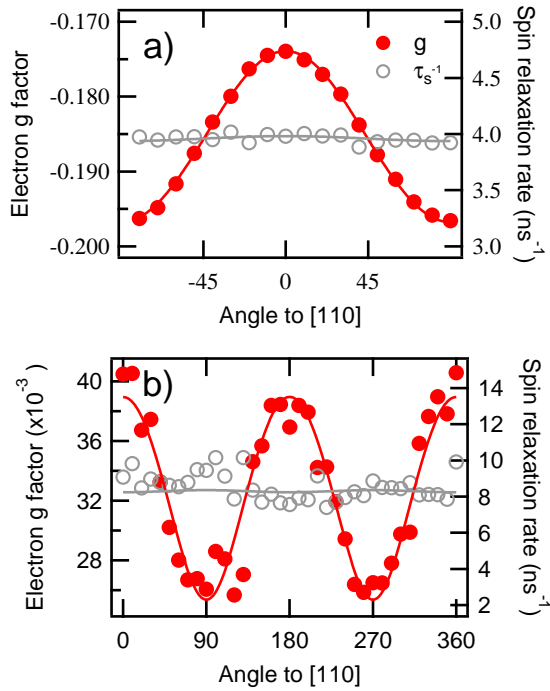


FIG. 2: (Color online) Extracted spin relaxation rate and electron g -factor for different magnetic field orientations from fits to the spin quantum beat measurements for a) sample A at 125 K and b) sample B at 25 K.

due to strong valence band mixing and k dependent spin splitting. The polarized luminescence is spectrally and temporally resolved by a spectrometer and a synchroscan streak camera with two-dimensional readout which provides a resolution of 0.5 nm and 8 ps, respectively. The degree of circular polarizations of the PL, which is proportional to the electron spin polarization, is measured by a switchable liquid crystal retarder and a polarizer.

Figure 1(c) depicts the time evolution of the degree of circular polarization for sample A at 3 T and 125 K for an in-plane magnetic field B along [110] and $[1\bar{1}0]$ directions. The observed oscillations are electron spin quantum beats the frequency being $\omega_L = g\mu_B\hbar^{-1}B$ and so a direct measure of g for the particular magnetic field direction [9]. Measurements of beats in $\langle S_z \rangle$ in this way do not yield the sign of g but a comparison with previous measurements on symmetric QWs identifies that g is negative for samples A, C, and D and positive for sample B [10, 18]. The two clearly distinct oscillation frequencies in Fig. 1(c) directly demonstrate the in-plane g anisotropy whereas the nearly identical decay of the two polarisation transients indicate that Γ_s is very nearly isotropic.

Figure 2 shows in more detail the dependence of g and Γ_s on the direction of magnetic field in samples A and B. The black (red online) solid curves in Fig. 2 depict fits of the anisotropy of g using Eq. 3 which directly yield both g_{xx} and g_{yy} . The diagonal components of the g -tensor

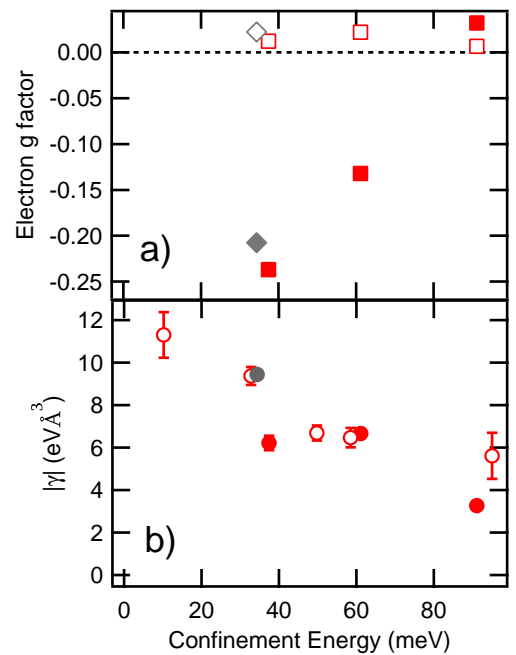


FIG. 3: a) (Color online) Variation in g_{xx} (solid squares) and g_{yy} (open squares) with confinement energy for samples B-C (5-25 K) and sample A (25 K) (grey diamonds). b) Experimental values of the Dresselhaus spin splitting constant against confinement energy (solid circles); open circles correspond to data from Ref. [19]

$g_{xx} = g_{yy}$ have been previously investigated in symmetrical quantum wells where the dependence on well width, i.e., confinement energy and barrier penetration, is well described by k-p theory [18, 20]. The solid squares in figure 3(a) show g_{xx} for all four samples confirming a similar strong dependence of g_{xx} on confinement energy for asymmetric QWs. The open squares in Fig. 3(a) show g_{yy} and these values yield by Eq. 2 the dependence of the Dresselhaus spin splitting constant γ on confinement energy (solid dots in Fig. 3(b)). The excellent agreement with data from Ref. [19] illustrates clearly that g_{yy} provides an accurate measure of γ in asymmetric (001) quantum wells. The remaining deviations of γ from the trend probably result from differences between the actual and the nominal sample structures which lead to uncertainties in the calculation of the wavefunction asymmetry. The distinct decrease of γ with confinement energy is expected from k-p theory and has similar origin to the change of g_{xx} with confinement energy in Fig. 3(a) [19].

Next, we study in detail the anisotropy of the spin relaxation rate. The open circles in Fig. 2(a) and (b) depict $\Gamma_s(\phi)$ for sample A and B respectively and the grey solid curves are fits according to Eq. 4. Additional temperature and density dependent measurements confirm that the Dyakonov-Perel spin relaxation mechanism dominates Γ_s . The measurements clearly show that there

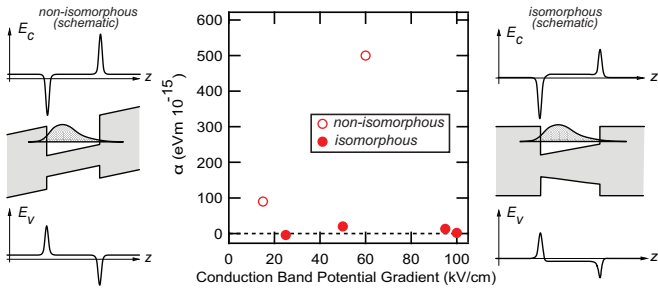


FIG. 4: (Color online) Extracted values of the Rashba spin-orbit constant vs. conduction band potential gradient for samples A-D (solid circles). The open circles show values for a built-in Hartree electric field [21] of ~ 15 kV/cm in an n-modulation doped structure and for an externally applied electric field of 60 kV/cm in an undoped (110)-oriented MQW sample [22]. Right and left panels show schematic potential profiles and electron probability density (middle) and effective electric field for conduction (top) and valence bands (bottom) (after [7]). For bound electrons, Ehrenfest's theorem forces the expectation value of the effective field in the conduction band to vanish. For an 'isomorphous' structure (right panel) the expectation value in the valence band will also vanish but *not* for a 'non-isomorphous' structure (left panel), giving zero (finite) SIA spin splitting for the former (latter) [8].

is almost no in-plane anisotropy of Γ_s and therefore α is close to zero even though the potential gradients in both samples are large (> 90 kV/cm).

Figure 4 compares α in our samples (solid circles) with previous experiments in external and internal (Hartree) electric fields (open circles) [21, 22]. The comparison of the measurements clearly show that the Rashba spin splitting in AlGaAs heterostructures is large even for a modest external (or internal) electric field but negligibly small in the case of asymmetries produced by alloy variation. Although allowed to be non-zero by the C_{2v} symmetry of the samples, the values of α which are required to fit the present data are zero within experimental uncertainties; they show both positive and negative values with no clear trend as a function of potential gradient and the fitted value of α/β is in all cases less than 0.1. The measurements push down by an order of magnitude the previous upper limit of Rashba spin splitting observed in samples with asymmetry from alloy variation [8]. The small values of α are a direct consequence of the 'isomorphous' band edges, that is the conduction and valence band potentials are related by a constant factor. This is due to the fact, that the expectation value of the effective electric field always vanishes in the conduction band due to Ehrenfest's theorem [7] *and* in 'isomorphous' structures as illustrated in the right hand panel of figure 4, will also vanish in the valence band and it is the latter which determines the spin splitting.

In conclusion, we have determined simultaneously the absolute values for the Dresselhaus and the Rashba spin-orbit interaction in undoped low-symmetry (001) quan-

tum wells. All samples show a distinctive anisotropy of the electron g-factor but essentially isotropic spin relaxation rates. This difference highlights the different origins of the two phenomena; the first is a measure of the conduction electron wavefunction asymmetry and the latter a measure of the expectation value of the valence band potential on conduction states. Although, a one sided-gradient of the conduction and/or the valence band leads in general to a finite Rashba spin-orbit interaction, the experiment proves that isomorphism of valence and conduction band in GaAs/AlGaAs quantum wells proscribe a sizeable, gradient-induced Rashba spin-orbit splitting.

We thank K. Köhler for providing us with the samples and W. W. Rühle for helpful discussions. We gratefully acknowledge financial support from Engineering and Physical Sciences Research Council (EPSRC) and from the Deutsche Forschungsgemeinschaft in the framework of the priority programm "SPP 1285 - Semiconductor Spintronics" and the excellence cluster "QUEST - Center for Quantum Engineering and Space-Time Research".

* Correspondence to: eldridge@nano.uni-hannover.de

- [1] F. Meier and B. Zakharchenya (eds.), *Optical Orientation*, volume 8 of *Modern Problems in Condensed Matter Science* (North-Holland Physics Publishing, Amsterdam, 1984).
- [2] E. L. Ivchenko and A. A. Kiselev, *Sov. Phys. Semicond.* **26**, 827 (1992).
- [3] M. I. Dyakonov and V. Y. Kachorovskii, *Sov. Phys. Semicond.* **20**, 110 (1986).
- [4] N. S. Averkiev and L. E. Golub, *Phys. Rev. B* **60**, 15582 (1999).
- [5] V. K. Kalevich and V. L. Korenev, *JETP Lett.* **57**, 571 (1993).
- [6] G. Dresselhaus, *Phys. Rev.* **100**, 580 (1955).
- [7] R. Winkler, *Spin-orbit Coupling Effects in Two-Dimensional Electron and Hole Systems* (Springer, Berlin, 2003).
- [8] P. S. Eldridge et al., *Phys. Rev. B* **82**, 045317 (2010).
- [9] A. P. Heberle, W. W. Rühle, and K. Ploog, *Phys. Rev. Lett.* **72**, 3887 (1994).
- [10] M. Oestreich et al., *IEEE J. Sel. Topics in Quantum Electron.* **2**, 747 (1996).
- [11] A. V. Larionov and L. E. Golub, *Phys. Rev. B* **78**, 4 (2008).
- [12] N. S. Averkiev et al., *Phys. Rev. B* **74**, 033305 (2006).
- [13] W. Hanle, *Zeitschrift für Physik A Hadrons and Nuclei* **30**, 93 (1924).
- [14] S. D. Ganichev et al., *Nature* **417**, 153 (2002).
- [15] S. D. Ganichev et al., *Phys. Rev. Lett.* **92**, 256601 (2004).
- [16] L. Meier et al., *Nature Phys.* **3**, 650 (2007).
- [17] M. Studer, S. Schön, K. Ensslin, and G. Salis, *Phys. Rev. B* **79**, 6 (2009).
- [18] M. J. Snelling et al., *Phys. Rev. B* **44**, 11345 (1991).
- [19] W. J. H. Leyland et al., *Phys. Rev. B* **76**, 195305 (2007).
- [20] R. M. Hannak et al., *Solid State Commun.* **93**, 313

(1995).

[21] D. Stich et al., Phys. Rev. B **76**, 073309 (2007).

[22] P. S. Eldridge et al., Phys. Rev. B **77**, 125344 (2008).